Real-Time Dynamic Robot-Assisted Hand-Object Interaction via Motion Primitives

Mingqi Yuan[1,2*], *Student Member, IEEE,* Huijiang Wang[1*], *Student Member, IEEE,*
Kai-Fung Chu[1], *Member, IEEE,* Fumiya Iida[1], *Senior Member, IEEE*, Bo Li[2],
Wenjun Zeng[3], *Fellow, IEEE*

Abstract—**Advances in artificial intelligence (AI) have been propelling the evolution of human-robot interaction (HRI) technologies. However, significant challenges remain in achieving seamless interactions, particularly in tasks requiring physical contact with humans. These challenges arise from the need for accurate real-time perception of human actions, adaptive control algorithms for robots, and the effective coordination between human and robotic movements. In this paper, we propose an approach to enhancing physical HRI with a focus on dynamic robot-assisted hand-object interaction (HOI). Our methodology integrates hand pose estimation, adaptive robot control, and motion primitives to facilitate human-robot collaboration. Specifically, we employ a transformer-based algorithm to perform real-time 3D modeling of human hands from single RGB images, based on which a motion primitives model (MPM) is designed to translate human hand motions into robotic actions. The robot's action implementation is dynamically fine-tuned using the continuously updated 3D hand models. Experimental validations, including a ring-wearing task, demonstrate the system's effectiveness in adapting to real-time movements and assisting in precise task executions.**

I. INTRODUCTION

The development of robotics and artificial intelligence (AI) has witnessed the revolution of the physical human-robot interaction (pHRI) [1]. With the ability to detect and react with its human partners, these robots have been applied in a range of scenarios including human-in-the-loop manipulation, robot-assistive dressing [2] and healthcare system such as the robot-assisted rehabilitation [3], medical treatment [4] and aged and children caring [5], [6]. In order to provide physical assistance to the human partners, these robots/agents are equipped with remarkable ability in sensing, manipulation, and autonomy, such that they can capture, interpret, and infer based on human cues and offer tangible support to the human. To date, one typical task to achieve sophisticated pHRI has spotlighted the hand-object interaction (HOI), where humans manipulate objects and interact with the environments [7], [8]. Recent developments in robotics have shed light on the robot-assisted HOI, such as using depth-enhanced vision systems and soft-robotic gloves to predict and assist with various hand postures for rehabilitation [9].

*These authors contributed equally to the work.
[1]Bio-Inspired Robotics Lab, Department of Engineering, University of Cambridge, Cambridge CB2 1PZ, UK. [2]Department of Computing, The Hong Kong Polytechnic University, Hong Kong SAR, CHN. [3]Eastern Institute of Technology, Ningbo, Zhejiang, CHN. `Corresponding author: Huijiang Wang, hw567@cam.ac.uk`

There are two fundamental technical challenges for robot-assisted HOI. One is hand pose estimation, which aims to accurately detect, track, and reconstruct the human hand in a dynamic environment under perturbation [10]. Research has focused on 3D human pose construction using diverse technologies such as wearable sensors, radio frequency (RF) technologies, and acoustic methods. For instance, [11] introduced a method that combines multi-view images with inertial measurement units (IMUs) attached to human limbs, significantly enhancing 2D pose estimation accuracy in occluded scenarios and integrating these estimates into a 3D model aligned with IMU data, thus improving overall pose estimation accuracy. In contrast, [12] developed "GoPose," a framework that estimates human poses by analyzing WiFi signals reflected off the body. This method operates with the existing WiFi infrastructure and does not require users to wear sensors, utilizing deep learning to transform WiFi signal characteristics into accurate 3D skeletal representations with an accuracy of approximately 4.7 cm across various scenarios, including non-line-of-sight conditions. Furthermore, [13] proposed a method for estimating human poses in 3D using only low-level acoustic signals, circumventing the need for high-level acoustic information such as speech. This method employs a convolutional neural network that utilizes phase and spectral features from acoustic signals captured by a single pair of microphones and loudspeakers, proving effective in various challenging environments. However, these methods have seen drawbacks regarding the indispensability of complex sensors, complexity of deployment, dependency on environmental conditions, and potential privacy concerns.

Another challenge lies in designing the robotic controller for robot-assisted manipulation. Various efforts have been put toward developing control interfaces, such as virtual joysticks [14], electromyography [15], IMUs [16], eye gaze detection [17] and brain-machine interfaces [18]. Among these, 3D hand gesture recognition [19], [20] has become the most popular method, serving as an end-to-end solution for humans to perform physical actions in the environment. In recent years, the development of 3D pose estimation based on single RGB images has become prevalent in the current HOI community due to its cheapness and ease of deployment. For instance, [21] leveraged the graph convolutional neural network (GCNN) to reconstruct the whole 3D mesh of the hand surface from a single RGB image, which can well represent hand shape variations and capture local details. [22] introduced a contact potential field (CPF) approach, treating interactions as a
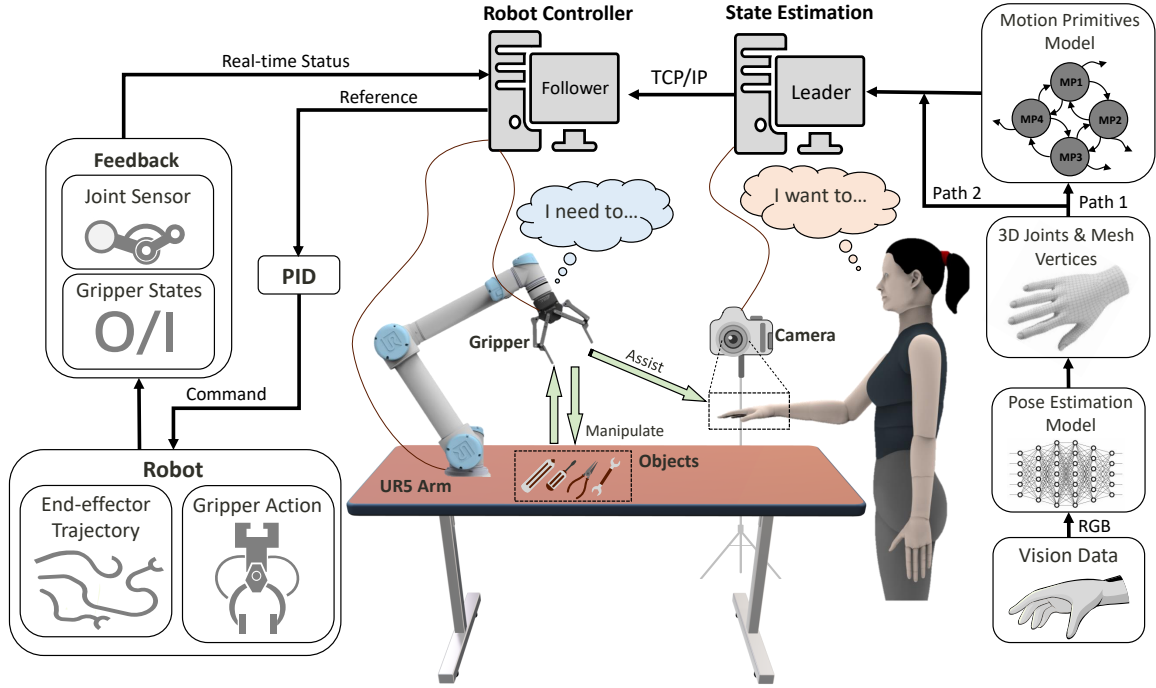
Fig. 1. Overview of the adaptive robotic system for robot-assisted hand-object interaction.

spring-mass system to allow for dynamic adjustments based on contact physics, which enhances the physical plausibility of hand-object interaction predictions, even in cases of significant discrepancies in ground-truth data. In contrast, [23] integrated the transformer architecture with graph convolution to create the MeshGraphormer, which adeptly captures both local and global interactions among mesh vertices and body joints. In summary, the computer vision (CV)-based approaches provide a cost-effective and end-to-end solution for capturing intricate hand movement that advances the design of pHRI platforms.

In this paper, we propose an adaptive robotic system for pHRI in the context of robot-assisted dressing. We introduced a robot controller based on motion primitives. This model enables autonomous robot motion and human-robot collaboration. The concept of motion primitive-based control follows a modular approach, allowing users to define various motions, resulting in more meaningful functioning. First, we introduced an RGB-based 3D hand pose estimation model and designed an adaptor to perform the real-time vibration-tolerant state estimation. By using the learning-based state estimation, we then proposed a closed-loop control architecture such that a robot arm and end-effector can adaptively adjust its motion to assist its human partners. Last, we introduce the action alignment model, which allows for the orientation of the end-effector and the human hand with a reasonable physical relative location and orientation. Experimental tests have validated the effectiveness of the designed hand pose module and the adaptive controller. Our proposed human-robot collaborative model can pave the way for future development of robot-assisted healthcare and medical treatment services.

II. RGB-BASED 3D HAND POSE SENSING

A key challenge to achieving efficient and robust robot-assisted HOI is accurately sensing and modeling the human hand in real-time. This involves acquiring the 3D coordinates of hand joints and the vertices of the hand surface, which are essential for hand localization and for providing references and feedback during robot actions. In this paper, we propose to leverage the 3D coordinates of hand joints to realize human intention recognition and adaptive control of robots. To that end, we incorporated a transformer-based pose estimation algorithm, MeshGraphormer [23], to perform real-time 3D perception and modeling of human hands based on RGB images. As shown in Figure 2, MeshGraphormer first leverages a pre-trained CNN to extract grid features and a global feature vector from the given RGB images. These features are then tokenized and fed to a multi-layer transformer-based encoder to output coarse mesh tokens, and a multi-layer perceptron (MLP) is utilized to perform upsampling to obtain full mesh tokens and mesh vertices. Finally, the 3D coordinates of hand joints are computed using a MANO model from [24]. Denote by F_{θ} the model of MeshGraphormer with network parameters θ, we have

$$(x, y, z) = F_{\theta}\left(P(I)\right), \tag{1}$$

where I is a raw RGB image, x, y, z are 3D coordinates vectors, and $P(\cdot)$ denotes the image preprocessing operation including resizing, cropping, normalizing, etc.

In practice, data oscillation may occur due to slight hand shaking during real-time detection, leading to unstable localization. To address the problem, we leverage the following
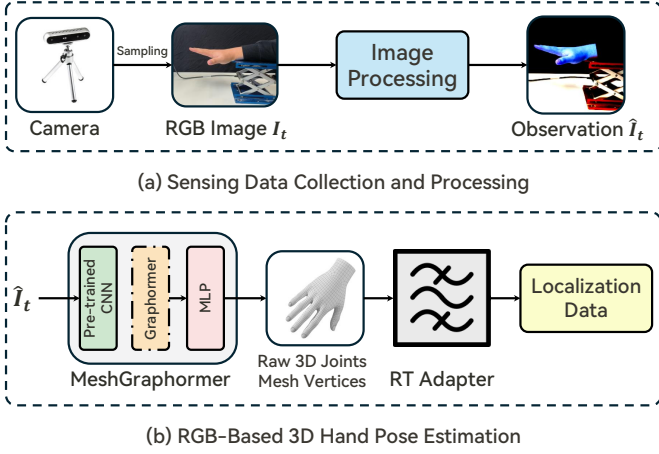
(a) Sensing Data Collection and Processing

(b) RGB–Based 3D Hand Pose Estimation

Fig. 2. Overview of the module for RGB-based and 3D hand pose estimation.

moving average filter to smooth the detection data:

$$\tilde{x}_t = \frac{1}{W} \sum_{i=t-W+1}^{t} x_i,$$
$$\tilde{y}_t = \frac{1}{W} \sum_{i=t-W+1}^{t} y_i, \qquad (2)$$
$$\tilde{z}_t = \frac{1}{W} \sum_{i=t-W+1}^{t} z_i,$$

where W is the sliding window size. Additionally, we implement asynchronous processing pipelines to optimize our system responsiveness and minimize latency in real-time applications for image preprocessing and pose estimation. Moreover, the hand pose estimation model can be replaced by a body pose model in our system, allowing the system to be adapted for full-body interaction scenarios. This flexibility is essential in complex environments where understanding hand and body gestures can significantly enhance the robot's ability to interpret human intentions accurately.

III. MOTION PRIMITIVES MODEL

For robot-assisted HOI, it is crucial to capture and precisely respond to changes in human intentions and provide appropriate feedback. In scenarios where a robot and a human collaboratively hold an object, the robot must continually monitor the human hand posture to sense their intentions and adapt its behavior, such as adjusting grip strength or orientation. However, it is consistently difficult to directly construct an effective mapping between human intentions and robot actions. To address the problem, we propose a motion primitives model (MPM) that converts human hand motions into robotic actions in real time. By utilizing the 3D coordinates information of hand joints, our model interprets and translates specific hand movements into corresponding mechanical responses. Specifically, we define a set of motion primitives of different levels. For example, low-level primitives such as moving forward, backward, and holding do not require additional reference information. In contrast, high-level primitives, like complex hand gestures indicating directional
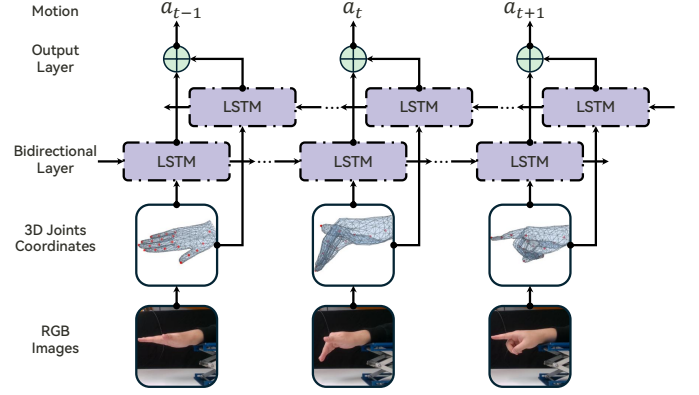
changes or speed adjustments, integrate contextual data from the environment and other sensors to enhance interaction. This layered approach allows the MPM to adaptively respond to diverse human intentions, enabling smoother and more intuitive human-robot collaboration.

We build the MPM using a bidirectional long short-term memory (LSTM) network [25], a type of recurrent neural network (RNN) particularly suited for sequence prediction problems. This choice is critical as it enables the model to retain context over time, which is essential for interpreting continuous and dynamic hand gestures. The LSTM network is trained on a self-collected dataset of hand motion sequences to encompass a spectrum of potential gestures and their corresponding robotic actions. Through this training, the network learns the individual gestures and their transitions, ensuring a fluid and intuitive control flow. Denote by M_ϕ the MPM with network parameters ϕ, we have

$$a_t = M_\phi(\{x_i, y_i, z_i\}_{i=t-N+1}^{t}), \qquad (3)$$

where a_t is the predicted probability distribution of motions, $a_t = \arg\max_i a_t[i]$ will be the output motion class, and N is a fixed sequence length. Meanwhile, the cross entropy [26] is selected as the loss function to train the MPM:

$$L(\phi) = -\sum_{i=1}^{T} \sum_{k=1}^{K} \hat{a}_t[k] \log(a_t[k]), \qquad (4)$$

where T is the number of time steps in the sequence, K is the number of possible actions, and $\hat{a}_t[k]$ is the ground truth indicator for class k at time t (1 if the class label k is the correct classification for t, and 0 otherwise).

In real-time detection, since the time it takes to complete a human hand motion is uncertain, the prediction results will change suddenly during the motion. In order to ensure the credibility of the recognition results, we use the following filter:

$$a_t = \begin{cases} a_t, & \text{Var}(A) = 0, |A| = N \\ \inf, & \text{else} \end{cases} \qquad (5)$$

where A is a queue of length N that stores the real-time results from MPM, $|A|$ is the number of stored results, and $\text{Var}(\cdot)$ is the variance (0 when all the results are identical).

Fig. 3. Workflow of the proposed MPM. Here, the extraction of 3D joints coordinates is performed by the module in Figure 2.

Finally, we would like to highlight the advantages of the proposed MPM. First, MPM directly uses the 3D coordinate sequences of hand joint points as input, which maximizes the difference between different gestures in the feature space and effectively improves the detection accuracy and robustness of the model. MPM requires few training data and demonstrates strong generalization capabilities. For instance, a model trained on data from a single human hand can successfully recognize unknown human hands, as demonstrated in the experimental section.

IV. ROBOT CONTROL

In the context of pHRI scenarios, CV-based hand recognition serves as the primary method for estimating the state of the hand to control the robot. In this section, we introduce the controller architecture designed for implementing hand-object interaction tasks.

A. Experimental Setup

In our experiments, we utilize the UR5 manipulator as the robotic arm and a two-finger RobotiQ gripper as the end-effector to execute pick-and-place tasks. Hand pose recognition is facilitated by an RGB camera (Intel RealSense). To simulate real-world scenarios, we use a ring object intended to be worn on a human finger as the item to be picked up. The experimental setup is illustrated in Figure 4.
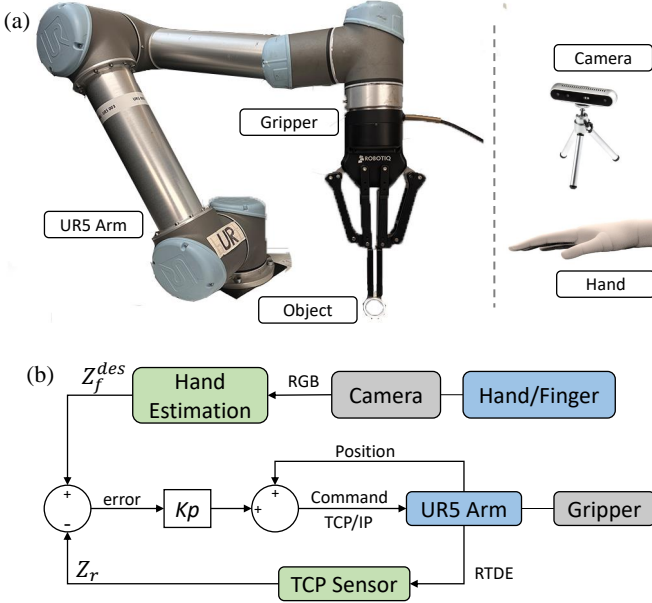

Fig. 4. The systematic framework of the hand-object interaction. (a) The robot setup includes a UR5 robotic arm equipped with a gripper for grasping objects. (b) The overall control architecture.

For controlling the UR5, we employed the real-time data exchange (RTDE) control interface to enable real-time manipulation of the tool center point (TCP) of the robot arm. Real-time control was achieved using the *servoL* function, ensuring a frame rate of 500 Hz. As a safety precaution during implementation, we configured a safety zone around the end-effector to mitigate the risk of potential human injury.

B. Controller Architecture

The interaction between the hand and the object requires the robot to exhibit adaptive behaviors based on human input, necessitating hierarchical control over the robot arm. This control is bifurcated into two components: control over the UR5 robot arm and control of the gripper.

The gripper control operates as an open-loop system, enabling the gripper to execute pinching and releasing actions on the object. Conversely, UR5 TCP control encompasses both open and closed-loop strategies. The open-loop control relies on predefined motion primitives. Upon program initialization, the camera and hand pose algorithm monitor hand movements and identify these primitives. When a motion primitive is detected, the robot executes predetermined incremental motions, allowing the user to adjust the spatial location of the TCP manually.

In contrast, real-time closed-loop control occurs during the cooperation stage. When the cooperation condition is triggered, the robot continuously approaches the human hand at a constant speed while tracking hand pose and receiving hand state information, such as finger angular deviation and fingertip location. Utilizing this data, the robot dynamically adjusts its vertical position and orientation to ensure successful object delivery. Throughout this process, the robot adapts both its spatial position and end-effector orientation to collaborate effectively with the human operator.

The transition between these control modes is triggered by the detection of specific motion primitives, *i.e.*, the "Ring" primitive, signaling the robot to enter a cooperation mode. The entire control architecture is depicted in Figure 4.

C. Action Alignment

In the context of HOI, a crucial aspect is the coordination between the object and the human. When the gripper holds the object, we treat the gripper-object system as a rigid body, assuming consistent pinching poses for multiple grasping actions. During the cooperation stage, where the gripper moves towards the human finger, the controller dynamically adjusts to accommodate finger bending and environmental perturbations. We propose an action alignment model to enable real-time adjustment of the robot's end-effector pose.
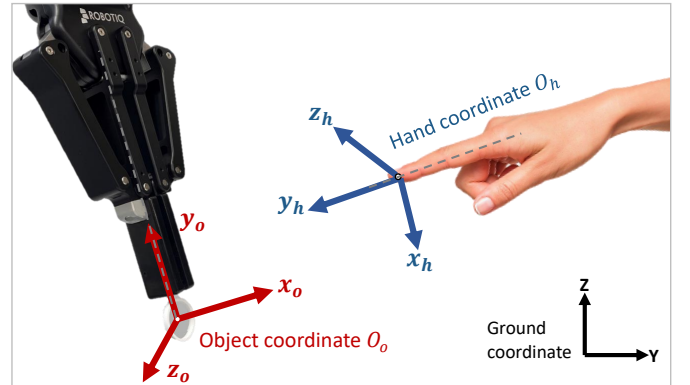

Fig. 5. The spatial coordinates alignment between the hand and object.

Hand Motion	RGB Image	Robot Action
Keep		Remains at the current location.
Switch		MP switch to TCP movement.
Come		Moves towards the hand.
Back		Moves away from the hand.
Ring		MP switches to adaptive orientation.

In Figure 5, we assume the spatial coordinates of both the UR5 robot's base and the human hand. Utilizing TCP-based real-time control, we define the spatial coordinate of the object as $O_o = [X_o, Y_o, Z_o]$. The center is established at the object's center, with the x-axis aligned to the object's normal direction. The y-axis corresponds to the gripper's central line, while the z-axis follows the right-hand rule. Similarly, with the employed hand pose recognition algorithm, we determine the fingertip's coordinate as $O_h = [X_h, Y_h, Z_h]$. The hand coordinate system originates from the fingertip, with the y-axis aligned with the fingertip's direction. The x-axis is positioned perpendicular to the y-axis and towards the bending side. The z-axis is set based on the right-hand rule. For the two coordinate systems defined in this initial system, it is always possible to find a rotation matrix $\mathbf{T}$ that performs the transformation from O_o to the O_h:

$$O_h = \mathbf{T} \cdot O_o. \tag{6}$$

In order to align the object with the finger, the object-based body coordinate should be aligned accordingly. For the given pointing pose in Figure 5, to ensure the aligned orientation we first compute the spatial angular deviations as:

$$\begin{aligned} \alpha &= \cos^{-1}\langle x_o, y_h \rangle \\ \beta &= \cos^{-1}\langle y_o, z_h \rangle. \end{aligned} \tag{7}$$

To ensure that the ring can be worn on the finger the orientation should follows:

$$x_g^o - x_g^h = 0 \tag{8}$$
$$y_g^h - y_g^o = v_h \cdot t \tag{9}$$
$$z_g^h - z_g^o = v_v \cdot t \tag{10}$$
$$\alpha = -1 \tag{11}$$
$$\beta = 1 \tag{12}$$

The subscript indicates the coordinate system being referenced, while the superscript indicates the object (ring or finger). The symbols v_h and v_v represent the robot's velocity in the horizontal and vertical directions, respectively.

This implies that in the process of human-robot cooperation, two objectives are satisfied. Firstly, as the human hand moves vertically, the robot's TCP adjusts correspondingly. Secondly, when there is a bending motion in the finger, the robot's TCP adapts its position to align the object with the central axis of the fingertip.

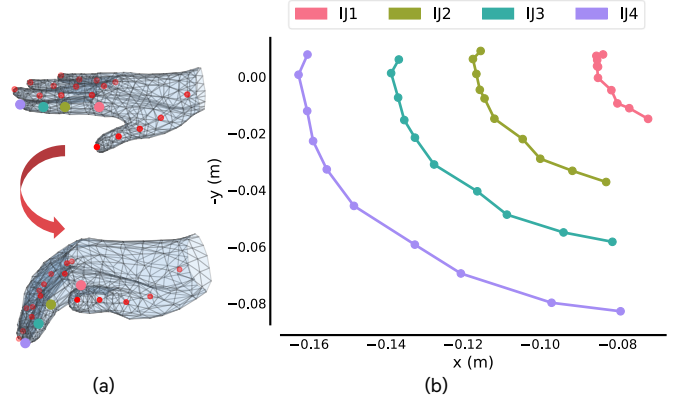## V. RESULTS

A. Hand Recognition Performance

(a)　(b)

Fig. 6. 3D modeling of the process of converting from the motion "Keep" to the motion "Come". (a) Mesh reconstruction of the hand motion, in which the filled circles represent the joints. (b) Changes of the coordinates of joints during the motion conversion process. Here, "IJ1-4" denotes the four joints of the index finger, respectively.

We first evaluate the effectiveness of the designed 3D hand pose module. Figure 6 demonstrates the 3D modeling of the transition process between two distinct hand motions. In the "Keep" motion, the y-axis coordinates of the four joints remain relatively unchanged. In contrast, during the transition to the "Come" motion, the x-axis coordinates of these joints progressively align. These observations indicate that our 3D hand pose module can accurately capture and model the hand motion changes, providing reliable reference information for the subsequent robot control.

B. MPM Training

1) Data Preparation: Table I illustrates the pre-defined motion primitives for the proposed ring-wearing task. For each motion, we asked the subject to make and maintain the motion and then collected 2000 consecutive frames of RGB image data, and the subject could make slight motion adjustments during the collection process. Then, these frames were used to extract 3D coordinates of 21 hand joints using the aforementioned pose estimation model. For a single trajectory, we sampled every 10 frames and intercepted a sequence of length 10. As a result, a motion dataset with 1000 samples was obtained, and the date shape of each input is $(10, 63)$. Furthermore, we use stratified sampling to divide the data set into a training set (80%) and a validation set (20%) to ensure that each type of action has the same number of samples.

2) Model Training: For the MPM, we leveraged a bidirectional LSTM with 2 recurrent layers, and the input size is (10, 63), and the number of features in the hidden state is 64. The LSTM is followed by a fully connected layer that maps the LSTM output to 5 classes corresponding to different hand motions and a softmax function to output the probability distribution over these classes. We trained the MPM for 100 epochs using a learning rate of 0.00025 and a batch size of 512, and Figure 7 illustrates the model performance changes during training. It can be seen that the model converges quickly and has good generalization performance.
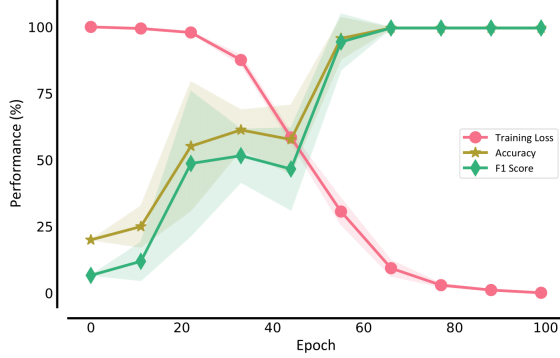

Fig. 7. The MPM performance versus training epochs. Accuracy is calculated as the ratio of correctly predicted observations to the total observations, and F1 score is a harmonic mean of precision and recall. The solid line and shaded regions represent the mean and standard deviation computed with five random seeds, respectively.

C. MPM-based Control and Adaptive Pose Adjustment

1) Motion Primitives Transition: The MPM has been proposed to initiate specific action sets for controlling the robot. Each motion primitive is activated individually. Figure 8 illustrates the motion control using the MPM. In this particular task, the motion of the UR5 along the y-axis is mainly controlled by two motion primitives (supporting Video S1). The robot demonstrates a good dynamic response to the PM commands. In this test scenario, a MP command signal of '1' corresponds to the 'Come' motion, where the robot approaches the human hand, while a MP command of '2' signifies a backward motion. The alignment between the detection of the MP command and the y-axis motion showcases effective control of the UR5 robot using the MPM. Note that this example focuses on MPM-based control of motion in one direction. However, the MPM can be expanded to enable similar control over other directional motions, offering versatility in robot control.

2) Adaptive Orientation: In a robot-assisted dressing task, the robot handles environmental and human-induced disturbances. Figure 9 shows the robot's Z-axis displacement and X-axis angular displacement trajectory. Over 30 seconds, the human bends and then lifts the index finger (see supporting Video S2). During this movement, the robot maintains its grip on the object (ring) and adjusts its TCP orientation in terms of vertical height and pointing angle. The robot achieves a maximum displacement of ΔZ of 74.23 mm and a rotational angle of 18.0 degrees. These adjustments enable the robot
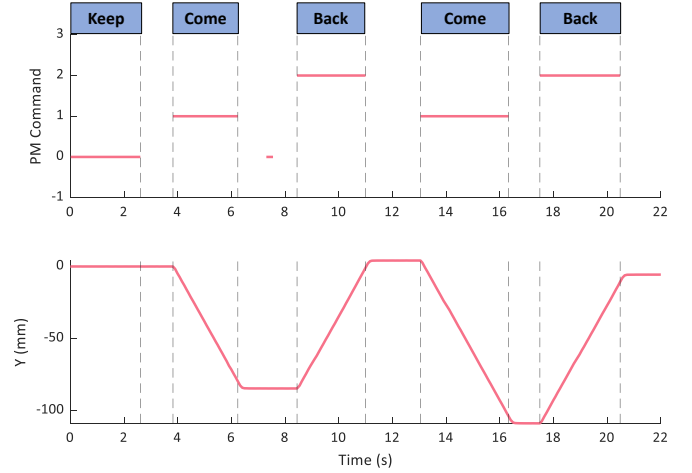

Fig. 8. The MPM and the control of UR5 arm motion. (a) The PM model is detected by the hand recognition algorithm, and (b) the corresponding motion of the UR5 robot arm in the Y-axis (horizontal) direction.

to maintain a suitable position for dressing, validating the effectiveness of the adaptive controller for action alignment discussed in Section IV-C. Note that the robot's action amplification ratio can be modified to adjust the level of its reactive behavior.

D. Robot-assisted Ring Wearing

The proposed hand pose estimation and adaptive controller have undergone real-world testing within a robot-assisted dressing task, specifically focusing on a ring-wearing scenario. In this task, the assistive robot is tasked with picking up a ring. Once the object is pinched, the motion of the robot is passively controlled using the MPM, allowing the human to fine-tune the initial positioning for collaboration. Subsequently, triggered by the MPM also, the robot transitions into the dynamic
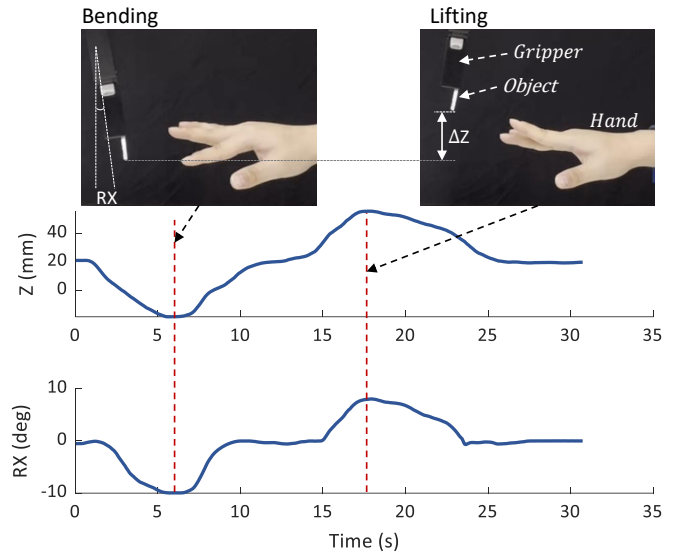

Fig. 9. The adaptive orientation of the UR5 robot arm according to the human input.
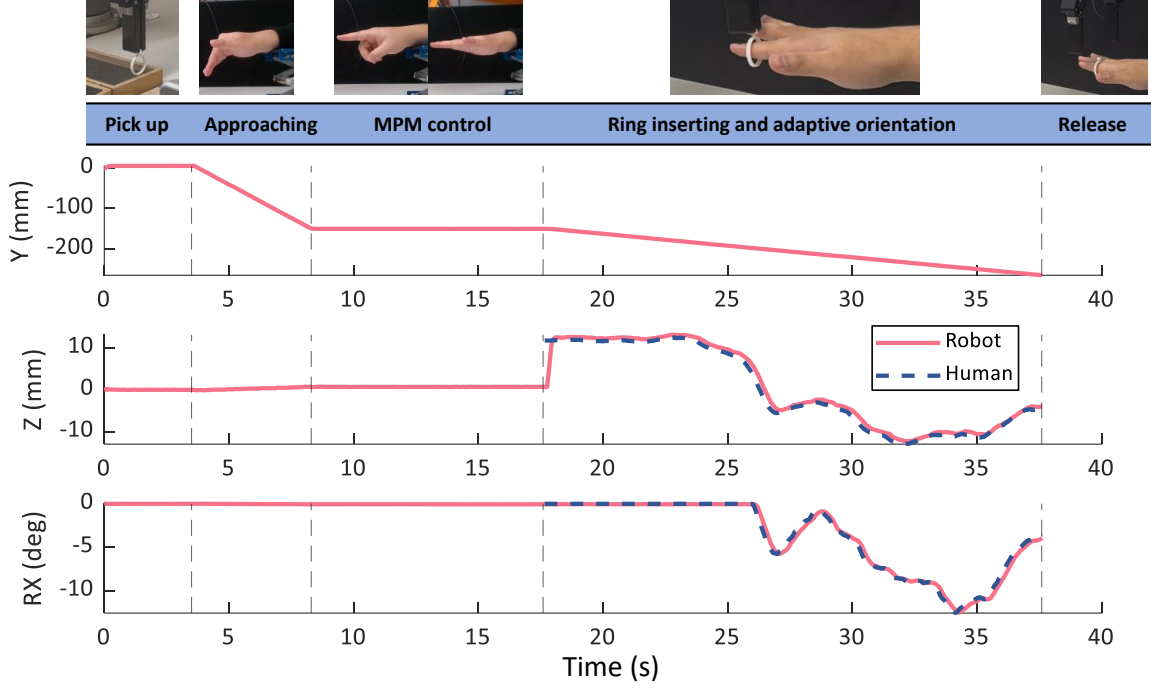
Fig. 10. The real-world performance of the robot-assisted dressing task in the context of ring-wearing.

cooperation stage. The robot actively responds to perturbations in hand pose, engaging in collaborative efforts to complete the task of wearing the ring.

Figure 10 illustrates the performance of the robot-assisted ring-wearing task (supporting Video S3). The first and second rows of curves represent the Y-axis and Z-axis motions of the TCP, while the third row depicts the angular displacement around the x-axis, corresponding to the ground coordinate in Figure 5.

Initially, the robot executes a pre-programmed action to pick up the ring. Subsequently, it is controlled by the MPM model, allowing the human operator to guide the end-effector's approach using the 'Come' hand pose. Once the operator determines the desired location, they initiate the 'Ring' motion primitive, transitioning the robot from passive control to active cooperation. From this point (17.6s) onwards, the robot maintains constant movement towards the hand while dynamically compensating for perturbations imposed by the human hand. The dashed blue curve denotes the motion of the CV-based hand pose estimation. As the human adjusts their finger position or location, the robot responds accordingly, ensuring correct ring orientation until successful delivery. At 37.5 seconds, the robot completes the ring-wearing task by releasing the ring, marking the task's conclusion, and validating the efficiency of the robot in real-world scenarios such as robot-assisted dressing.

VI. CONCLUSION

In this paper, we proposed an adaptive robotic system for robot-assisted hand-object interaction (HOI). We presented a learning-based state estimation that integrates the real-time 3D construction of hand pose. An RNN model has been trained to learn human hand motions. This is used as the motion primitives, which are translated into pre-defined robotic actions in a contactless manner. On the other side, we have designed a closed-loop controller that enables the spatial alignment between the end-effector and the fingering, ensuring that the object is manipulated in the desired way.

In the case study of a ring-wearing task, the adaptive robotic system demonstrates its effectiveness in assisting its human teammate and the robustness against environmental perturbations. Future work can be developed to expand the motion primitive sets and refine interaction dynamics, enhancing the applications of pHRI systems in practical environments.

ACKNOWLEDGMENT

ETHICS STATEMENT

This study involving human participants was conducted in accordance with the principles embodied in the Declaration of Helsinki and local statutory requirements. The research protocol was approved by the Research Ethics Committee of the Department of Engineering, University of Cambridge.

REFERENCES

[1] M. Soori, B. Arezoo, and R. Dastres, "Artificial intelligence, machine learning and deep learning in advanced robotics, a review," *Cognitive Robotics*, 2023.

[2] F. Zhang and Y. Demiris, "Learning garment manipulation policies toward robot-assisted dressing," *Science robotics*, vol. 7, no. 65, eabm6010, 2022.

[3] Q. Ai, Z. Liu, W. Meng, Q. Liu, and S. Q. Xie, "Machine learning in robot assisted upper limb rehabilitation: A focused review," *IEEE Transactions on Cognitive and Developmental Systems*, 2021.

[4] H. Su, A. Di Lallo, R. R. Murphy, R. H. Taylor, B. T. Garibaldi, and A. Krieger, "Physical human–robot interaction for clinical care in infectious environments," *Nature Machine Intelligence*, vol. 3, no. 3, pp. 184–186, 2021.

[5] K. Wada, T. Shibata, T. Saito, and K. Tanie, "Effects of robot-assisted activity for elderly people and nurses at a day service center," *Proceedings of the IEEE*, vol. 92, no. 11, pp. 1780–1788, 2004.

[6] D. Feil-Seifer and M. J. Matarić, "Socially assistive robotics," *IEEE Robotics & Automation Magazine*, vol. 18, no. 1, pp. 24–31, 2011.

[7] H. Fan, T. Zhuo, X. Yu, Y. Yang, and M. Kankanhalli, "Understanding atomic hand-object interaction with human intention," *IEEE Transactions on Circuits and Systems for Video Technology*, vol. 32, no. 1, pp. 275–285, 2021.

[8] L. Yang, K. Li, X. Zhan, *et al.*, "Oakink: A large-scale knowledge repository for understanding hand-object interaction," in *Proceedings of the IEEE/CVF Conference on Computer Vision and Pattern Recognition*, 2022, pp. 20 953–20 962.

[9] E. Rho, H. Lee, Y. Lee, *et al.*, "Multiple hand posture rehabilitation system using vision-based intention detection and soft-robotic glove," *IEEE Transactions on Industrial Informatics*, 2024.

[10] C. Zimmermann and T. Brox, "Learning to estimate 3d hand pose from single rgb images," in *Proceedings of the IEEE international conference on computer vision*, 2017, pp. 4903–4911.

[11] Z. Zhang, C. Wang, W. Qin, and W. Zeng, "Fusing wearable imus with multi-view images for human pose estimation: A geometric approach," in *Proceedings of the IEEE/CVF Conference on Computer Vision and Pattern Recognition*, 2020, pp. 2200–2209.

[12] Y. Ren, Z. Wang, Y. Wang, S. Tan, Y. Chen, and J. Yang, "Gopose: 3d human pose estimation using wifi," *Proceedings of the ACM on Interactive, Mobile, Wearable and Ubiquitous Technologies*, vol. 6, no. 2, pp. 1–25, 2022.

[13] Y. Shibata, Y. Kawashima, M. Isogawa, G. Irie, A. Kimura, and Y. Aoki, "Listening human behavior: 3d human pose estimation with acoustic signals," in *Proceedings of the IEEE/CVF Conference on Computer Vision and Pattern Recognition*, 2023, pp. 13 323–13 332.

[14] A. Campeau-Lecours, U. Côté-Allard, D.-S. Vu, F. Routhier, B. Gosselin, and C. Gosselin, "Intuitive adaptive orientation control for enhanced human–robot interaction," *IEEE Transactions on robotics*, vol. 35, no. 2, pp. 509–520, 2018.

[15] C. L. Fall, G. Gagnon-Turcotte, J.-F. Dube, *et al.*, "Wireless semg-based body–machine interface for assistive technology devices," *IEEE journal of biomedical and health informatics*, vol. 21, no. 4, pp. 967–977, 2016.

[16] S. Jain, A. Farshchiansadegh, A. Broad, F. Abdollahi, F. Mussa-Ivaldi, and B. Argall, "Assistive robotic manipulation through shared autonomy and a body-machine interface," in *2015 IEEE international conference on rehabilitation robotics (ICORR)*, IEEE, 2015, pp. 526–531.

[17] M. Leroux, M. Raison, T. Adadja, and S. Achiche, "Combination of eyetracking and computer vision for robotics control," in *2015 IEEE International Conference on Technologies for Practical Robot Applications (TePRA)*, IEEE, 2015, pp. 1–6.

[18] T. Lampe, L. D. Fiederer, M. Voelker, A. Knorr, M. Riedmiller, and T. Ball, "A brain-computer interface for high-level remote control of an autonomous, reinforcement-learning-based robotic system for reaching and grasping," in *Proceedings of the 19th international conference on Intelligent User Interfaces*, 2014, pp. 83–88.

[19] J. Kofman, X. Wu, T. J. Luu, and S. Verma, "Teleoperation of a robot manipulator using a vision-based human-robot interface," *IEEE transactions on industrial electronics*, vol. 52, no. 5, pp. 1206–1219, 2005.

[20] Q. Gao, Y. Chen, Z. Ju, and Y. Liang, "Dynamic hand gesture recognition based on 3d hand pose estimation for human–robot interaction," *IEEE Sensors Journal*, vol. 22, no. 18, pp. 17 421–17 430, 2021.

[21] L. Ge, Z. Ren, Y. Li, *et al.*, "3d hand shape and pose estimation from a single rgb image," in *Proceedings of the IEEE/CVF Conference on Computer Vision and Pattern Recognition*, 2019, pp. 10 833–10 842.

[22] L. Yang, X. Zhan, K. Li, W. Xu, J. Li, and C. Lu, "Cpf: Learning a contact potential field to model the hand-object interaction," in *2021 IEEE/CVF International Conference on Computer Vision (ICCV)*, 2021, pp. 11 077–11 086.

[23] K. Lin, L. Wang, and Z. Liu, "Mesh graphormer," in *Proceedings of the IEEE/CVF international conference on computer vision*, 2021, pp. 12 939–12 948.

[24] J. Romero, D. Tzionas, and M. J. Black, "Embodied hands: Modeling and capturing hands and bodies together," *ACM Transactions on Graphics, (Proc. SIGGRAPH Asia)*, 245:1–245:17, vol. 36, no. 6, Nov. 2017.

[25] S. Hochreiter and J. Schmidhuber, "Long short-term memory," *Neural computation*, vol. 9, no. 8, pp. 1735–1780, 1997.

[26] T. M. Cover, *Elements of information theory*. John Wiley & Sons, 1999.